

# Importance of Translation–Replication Balance for Efficient Replication by the Self-Encoded Replicase

Norikazu Ichihashi,<sup>[a]</sup> Tomoaki Matsuura,<sup>[a]</sup> Hiroshi Kita,<sup>[b]</sup> Kazufumi Hosoda,<sup>[a]</sup> Takeshi Sunami,<sup>[b]</sup> Koji Tsukada,<sup>[c]</sup> and Tetsuya Yomo<sup>\*[a, b, d]</sup>

*In all living systems, the genetic information is replicated by the self-encoded replicase (Rep); this can be said to be a self-encoding system. Recently, we constructed a self-encoding system in liposomes as an artificial cell model, consisting of a reconstituted translation system and an RNA encoding the catalytic subunit of Q $\beta$  Rep and the RNA was replicated by the self-encoded Rep produced by the translation reaction. In this system, both the ribosome (Rib) and Rep bind to the same RNA for translation and replication, respectively. Thus, there could be a dilemma: effective*

*RNA replication requires high levels of Rep translation, but excessive translation in turn inhibits replication. Herein, we actually observed the competition between the Rib and Rep, and evaluated the effect for RNA replication by constructing a kinetic model that quantitatively explained the behavior of the self-encoding system. Both the experimental and theoretical results consistently indicated that the balance between translation and replication is critical for an efficient self-encoded system, and we determined the optimum balance.*

## Introduction

The assembly of an artificial cell is an attractive approach to gain a deeper understanding of the essence of cellular systems and their origins on Earth<sup>[1–3]</sup> and will also provide unprecedented opportunities for biotechnology.<sup>[4]</sup> An advantage of using the artificial cell is its defined and controllable components, which enable the determination of operation principles of cellular systems under controlled conditions. Several researchers are engaged in attempts to assemble an artificial cell by two complementary approaches: the bottom-up and top-down approaches.<sup>[5]</sup> In the former, artificial cell models have been constructed with chemically simple components, such as fatty-acid membranes,<sup>[1,6–8]</sup> and ribozymes.<sup>[9,10]</sup> In the latter approach, artificial cells are being constructed from contemporary proteins or phospholipids. Several enzymatic reactions have been performed in liposomes or emulsions as artificial cell models,<sup>[11–17]</sup> and plans for a minimal gene set sufficient for self-replication have been presented.<sup>[2,18]</sup> Although the individual reactions are available in liposomes, the ability to coordinate them into an integrated system is still lacking.<sup>[4]</sup>

In either approach, one of the major challenges is the construction of a system for the replication of genetic information. In the bottom-up approach, replication by ribozymes has improved but is still limited.<sup>[19]</sup> In the top-down approach, gene replication by proteins in liposomes has been performed by externally added replication enzymes.<sup>[12,20]</sup> However, genetic information is replicated by the self-encoded replicase (Rep) in all living systems, which we term a self-encoding system. Recently, we constructed a self-encoding system in liposomes, which consisted of a sense RNA (S) that encoded the  $\beta$  subunit of RNA-dependent RNA polymerase of the Q $\beta$  phage (Q $\beta$  Rep) as the genetic information and a reconstituted translation system, in which all components were purified individually (Figure 1 A).<sup>[21]</sup> Q $\beta$  Rep is a heterotetramer composed of a  $\beta$  sub-

unit and three host proteins: ribosomal protein S1 and elongation factors Tu(EF-Tu) and Ts(EF-Ts). As all the host factors are included in the reconstituted translation system, mature Q $\beta$  Rep is generated by providing only the  $\beta$  subunit.<sup>[22]</sup> Hence, in this system, the  $\beta$  subunit of Q $\beta$  Rep is first synthesized from the sense RNA to form Q $\beta$  Rep, which then replicates the sense RNA by synthesis of complementary antisense RNA.

In the self-encoding system, the sense RNA participates in two reactions: translation of the Rep and replication of RNA. In such cases, these two reactions must be coordinated for efficient replication, because they can compete for the sense RNA, as reported in RNA phage,<sup>[23,24]</sup> where the ribosome (Rib) and Rep compete for the same genomic RNA. Thus, there could be a dilemma. More replication by self-encoded Rep would require higher levels of Rep expression, while excessive expres-

[a] Dr. N. Ichihashi, Dr. T. Matsuura, Dr. K. Hosoda, Prof. T. Yomo  
Department of Bioinformatics Engineering  
Graduate School of Information Science and Technology  
Osaka University, 2-1 Yamadaoka, Suita  
Osaka, 565-0871 (Japan)  
Fax: (+81) 6-6879-7433  
E-mail: yomo@ist.osaka-u.ac.jp

[b] Dr. H. Kita, Dr. T. Sunami, Prof. T. Yomo  
Exploratory Research for Advanced Technology (ERATO)  
Japan Science and Technology Agency (JST)  
2-1 Yamadaoka, Suita, Osaka, 565-0871 (Japan)

[c] Dr. K. Tsukada  
Department of Biotechnology  
Graduate School of Engineering, Osaka University  
2-1 Yamadaoka, Suita, Osaka, 565-0871 (Japan)

[d] Prof. T. Yomo  
Graduate School of Frontier Biosciences, Osaka University  
University 2-1 Yamadaoka, Suita, Osaka, 565-0871 (Japan)

Supporting information for this article is available on the WWW under <http://www.chembiochem.org> or from the author.

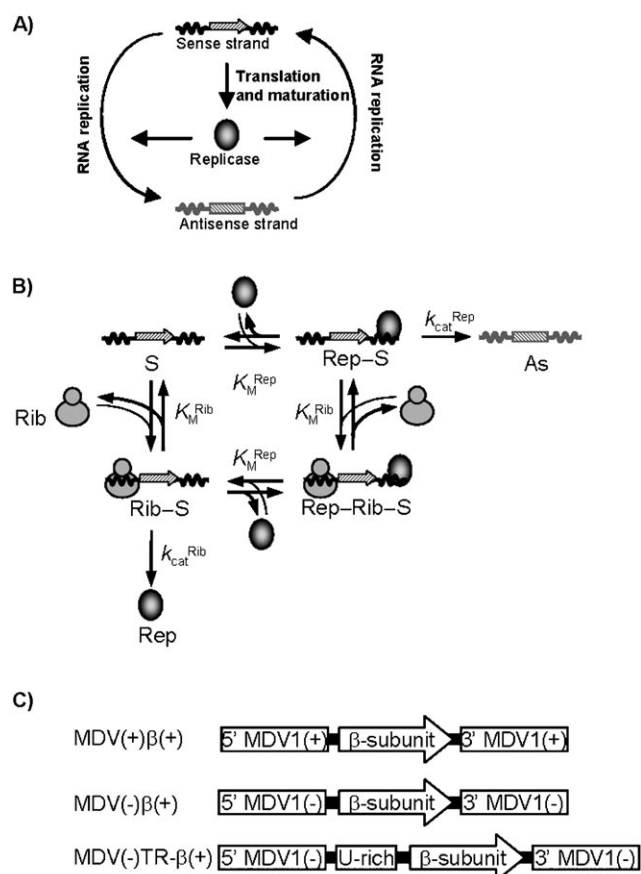


**Figure 1.** A) Scheme of the self-encoding system. Sense RNA serves as the genetic information. The catalytic subunit of RNA Rep is translated from sense RNA and matured by association with the components included in the reconstituted translation system. The matured Rep synthesizes the antisense strand and then the sense strand to complete the replication reaction. B) Scheme of the kinetic model. Ribosome (Rib) and replicase (Rep) bind sense RNA (S). These binding processes are assumed to be in equilibrium. The  $K_M^{Rib}$  and  $K_M^{Rep}$  are Michaelis constants, and  $k_{cat}^{Rib}$  and  $k_{cat}^{Rep}$  are the rate constants for translation by the Rib and antisense strand (As) synthesis by Rep, respectively. In this model, both As synthesis and translation from the Rep–Rib–RNA complex are neglected. C) Schematic representation of the sense strand RNAs. The sequence (ca. 1880 bases) of the  $\beta$  subunit of Q $\beta$  Rep was embedded in MDV-1(+) RNA or MDV-1(-) RNA (ca. 220 bases). A U-rich 15-mer sequence was added to MDV(-) $\beta$ (+) to produce MDV(-)TR- $\beta$ (+), which has a higher affinity for ribosomes.

sion triggered by binding of the Ribs, would inhibit replication. In this study, we examined whether there is competition between the Rib and Rep in our self-encoding system, and if so, what is the optimum Rib concentration for efficient replication. The answers to these questions will contribute not only to the construction of an artificial cell containing more efficient replication systems, but will also provide knowledge on how to coordinate different reaction systems into an integrated self-encoding system.

In the self-encoding system, we did, in fact, observe competition between the Rib and Rep for the sense RNA; increasing the Rib concentration facilitated translation, but excessive Rib levels inhibited replication, depending on the affinity of the Rib for the sense RNA. To quantitatively evaluate the effect of this competition on RNA synthesis, we constructed a kinetic

model that considered the competition between the Rib and the Rep for the sense RNA. The experimental results were explained well by the model and independently determined parameters. Furthermore, we established a strategy to estimate the optimum Rib concentration for the efficient replication of genetic information in an artificial cell.

## Results

### Kinetic model

We modified the previous kinetic model of Q $\beta$  Rep<sup>[25,26]</sup> (for details see the Supporting Information) to quantitatively describe the reactions in the self-encoding system, which include translation, antisense strand (As) synthesis and the competition between them (Figure 1 B). We evaluated As synthesis as an index of replication of the genetic information for convenience. The As is a copy of the genetic information, and its efficient synthesis is necessary for effective self-encoding replication. The kinetic model was composed of only one sense RNA, ribosomes (Ribs) and replicase (Rep) produced by the Ribs. The characteristic feature is the competition between the Rib and Rep. The competition effect observed is the inhibition of translation and replication when both the Rib and Rep bind to the same RNA (see below for details).

The Rib binds to the ribosome-binding sequence at the 5' end of the sense strand RNA (S). The Rep binds to the 3' end sequence—the start site of replication.<sup>[27]</sup> Thus, both the Rib and Rep bind to the same RNA to form a Rep–Rib–RNA complex (Rep–Rib–S), which we assumed was unable to produce full-length As or the Rep subunit.<sup>[23]</sup> The  $K_M^{Rib}$  and  $K_M^{Rep}$  are the Michaelis constants, they indicate the affinity of the sense RNA for the Rib and Rep, respectively;  $k_{cat}^{Rep}$  is the rate constant for As synthesis from the Rep–RNA complex (Rep–S), and  $k_{cat}^{Rib}$  is the rate constant for the translation of Rep from the Rib–RNA complex (Rib–S). The synthesis rates of Rep ( $V^{Rep}$ ) and As RNA ( $V^{As}$ ) were derived from this kinetic model based on the assumptions described below (see Experimental Section for derivations).

The total concentration of the sense strand RNA was assumed to remain constant during the reaction because sense strand synthesis was negligible over the experimental time-scale.<sup>[21]</sup> The concentration of single stranded sense RNA can be reduced by double-stranded RNA formation with the As. However, this was also negligible as the As was synthesized at a concentration only one tenth that of the sense strand (Figures S5 and S6). The binding of the Rib and Rep to the sense strand was assumed to occur substantially faster than the subsequent polymerization steps, which is consistent with previous observations,<sup>[28,29]</sup> and thus, binding was assumed to be at equilibrium.

### Parameter determination under noncompetitive conditions

According to the equations shown in the Experimental Section,  $V^{Rep}$  and  $V^{As}$  are represented as functions of parameters that can be determined experimentally. The parameters were deter-

mined individually under conditions in which there was no competition between the Rep and Rib. These conditions were achieved experimentally by employing an excess of the sense RNA relative to both the Rib and Rep. Under these conditions,  $V^{\text{Rep}}$  and  $V^{\text{As}}$  are written as Michaelis–Menten equations, which eases the experimental determination of the kinetic parameters (for details see Figures S1–S4). Thus, we determined the parameters for translation by Ribs ( $K_M^{\text{Rib}}$ ,  $k_{\text{cat}}^{\text{Rib}}$ ), for replication by Rep ( $K_M^{\text{Rep}}$ ,  $k_{\text{cat}}^{\text{Rep}}$ ), the active ratio of Rep ( $\alpha^{\text{Rep}}$ ) and the active ratio of Rib ( $\alpha^{\text{Rib}}$ ) independently under noncompetitive conditions for all three sense RNA sequences used (Table 1). The

Table 1. Kinetic parameters of the self-encoding system.				
	$K_M^{\text{Rep}}$ [nM]	$k_{\text{cat}}^{\text{Rep}}$ [min <sup>-1</sup> ]	$K_M^{\text{Rib}}$ [nM]	$k_{\text{cat}}^{\text{Rib}}$ [min <sup>-1</sup> ]
MDV(+) $\beta$ (+)	23 $\pm$ 9	0.25 $\pm$ 0.03	330 $\pm$ 40	0.035 $\pm$ 0.025 <sup>[a]</sup>
MDV(-) $\beta$ (+)	12 $\pm$ 5	0.25 $\pm$ 0.02	210 $\pm$ 20	0.014 $\pm$ 0.0004 <sup>[a]</sup>
MDV(-)TR- $\beta$ (+)	13 $\pm$ 4	0.18 $\pm$ 0.01	22 $\pm$ 3	0.044 $\pm$ 0.002

The active ratio of ribosomes ( $\alpha^{\text{Rib}}$ ) was estimated to be 0.17 ( $\pm$  0.02). The active ratios of Q $\beta$  replicase ( $\alpha^{\text{Rep}}$ ) were estimated to be 1.0 ( $\pm$  0.1), 0.64 ( $\pm$  0.09) and 1.1 ( $\pm$  0.1)–0.0014 ( $\pm$  0.0003)  $\times$  [Rib]<sub>i</sub> for MDV(+) $\beta$ (+), MDV(-) $\beta$ (+) and MDV(-)TR- $\beta$ (+), respectively. See Figures S3 and S4 for details. [a] In the presence of RNA synthesis (Figure 3C), 1.5-fold values were used.

parameters  $\alpha^{\text{Rep}}$  and  $\alpha^{\text{Rib}}$  are the fraction of Rep and Rib molecules, respectively, that are enzymatically active. The three sense RNA constructs are shown schematically in Figure 1C. MDV(+) $\beta$ (+) and MDV(-) $\beta$ (+) carry the Q $\beta$  Rep  $\beta$ -subunit sequence on the plus and minus strand, respectively, of the known, amplifiable RNA sequence, MDV-1.<sup>[30]</sup> MDV(-)TR- $\beta$ (+), which carries a 15-mer U-rich sequence insertion at the 5' end of the ribosome-binding sequence of the  $\beta$  subunit of MDV(-) $\beta$ (+), showed an increased affinity for the Rib (smaller  $K_M^{\text{Rib}}$ ) than did MDV(-) $\beta$ (+). Note that MDV(-)TR- $\beta$ (+) also showed a difference in the active ratio of the translated replicase,  $\alpha^{\text{Rep}}$ , which decreased when the Rib concentration was increased; the ratios for the other RNAs were almost constant (see the legends of Table 1 and Figure S4). Detailed procedures for parameter determination are described in the Supporting Information (Figures S1–S4).

### Comparison of theoretical prediction to experimental results under competitive conditions

From the equations shown in the Experimental Section and the parameters determined in the experiments in the absence of competition, we were able to predict the experimental results in the presence of competition, where RNA concentration was lower than the Rib concentration. In this case, the fraction of RNA bound by both the Rib and Rep increased, and thus the competition effect became significant. In the following sections, we describe the measurement of translation and As synthesis at a lower RNA concentration (70 nM) together with the results of

the comparison with the prediction. If these two outcomes are similar, then the results support the validity of the model. The theoretical predictions of  $V^{\text{Rep}}$  and  $V^{\text{As}}$  are relatively sensitive to  $\alpha^{\text{Rib}}$  and  $k_{\text{cat}}^{\text{Rep}}$ , respectively, but if these changes are within the experimental error then no significant changes to the theoretical predictions are necessary.

### Translation of Rep under competitive conditions

First, we measured the translation of the Rep  $\beta$  subunit in the absence of RNA synthesis; this was achieved by omitting UTP from the reaction mixture. In this experiment, Rep can bind to the sense strand, but cannot synthesize As. Here, the competition effect can exist because both the Rib and Rep can bind to the sense RNA, but the effect should be negligible because the Rib is in excess compared to the Rep. With all three RNAs, the time courses were linear until 60 min (Figure S5A), and the slopes are plotted in Figure 2 ( $\circ$ ). For MDV(+) $\beta$ (+) and MDV(-) $\beta$ (+), the translation rates increased linearly as the Rib concentration increased. For MDV(-)TR- $\beta$ (+), the translation rate was almost saturated at a Rib concentration of 450 nM.

Next, we measured the translation of the Rep  $\beta$  subunit in the presence of RNA synthesis when UTP was included (UTP+), and both translation and As synthesis by the translated Rep occurred simultaneously. The time courses were also linear until 60 min (Figure S5B), and the slopes are plotted in Figure 2 for each sense RNA ( $\Delta$ ). The translation rates in the presence of RNA synthesis (UTP+) were slightly higher than that in the absence of RNA synthesis (UTP-) for MDV(+) $\beta$ (+) and MDV(-) $\beta$ (+). A similar enhancement of translation was reported previously, which was explained as the newly synthesized sense RNA acting as an efficient template.<sup>[31]</sup> The theoretical predictions calculated from the equations and parameters (black line) were similar to the experimental results in the absence of RNA synthesis (UTP-) for all template RNAs. This similarity is reasonable because the parameters used for the prediction were determined in the absence of RNA synthesis. Taken together, the experimental results were explained well by our kinetic model and parameters in both the absence and presence of RNA synthesis differed from predicted values by

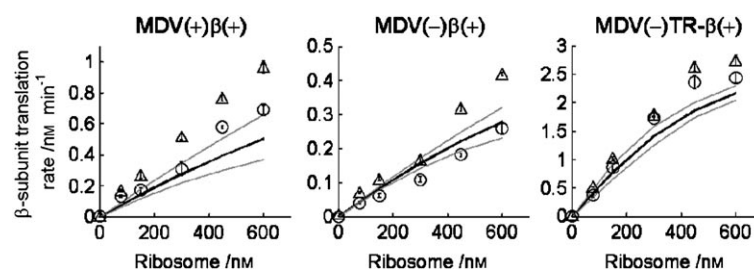


**Figure 2.** Replicase (Rep)  $\beta$ -subunit translation rate. Experimentally, the level of translated  $\beta$  subunit was measured at various Rib concentrations in the absence (UTP-,  $\circ$ ) or presence (UTP+,  $\Delta$ ) of RNA synthesis. The time-course curves (Figure S5) were subjected to linear regression and the slopes were plotted for each sense RNA. The error bars indicate standard errors. Theoretically, the translation rate was calculated from Equations (2) and (4), and the parameters shown in Table 1 (black line). Theoretically calculated values  $\pm$  standard deviation lines are also shown (gray lines; see the Supporting Information text for details).

less than twofold. The similarity of the experimental results to the theoretical predictions was not surprising because the competition effect should be negligible for the translation reaction due to the excess amount of Ribs relative to that of Rep. The enhancing effect was included in our model by a 1.5-fold increase in  $k_{\text{cat}}^{\text{Rep}}$  for MDV(+) $\beta$ (+) and MDV(-) $\beta$ (+) in the next section.

### Antisense strand (As) synthesis under competitive conditions

We measured As synthesis in the absence or presence of translation. In the absence of translation, serine and lysine, which are the second and third amino acid residues in the  $\beta$  subunit, respectively, were omitted, and purified Q $\beta$  Rep (20 nM) was added, the  $\alpha^{\text{Rep}}$  of which has been estimated to be 20%.<sup>[29]</sup> In this experiment, the competition effect should be observed as the Rib binds to the sense strand RNA. Because Q $\beta$  Rep is known to become inactivated at the late phase of the reaction,<sup>[29]</sup> we measured As synthesis only at the early phase, during which the time course remained linear (up to 9–12 min; Figure S6), and the slopes are plotted in Figure 3A (○). The As synthesis rates decreased slightly with increasing Rib concentration for MDV(+) $\beta$ (+) and MDV(-) $\beta$ (+) and markedly for MDV(-)TR- $\beta$ (+). The theoretical predictions showed a similar tendency (black line); this indicates that the model was able to adequately explain the competition effect.

Next, we examined whether the model could explain the results in the presence of translation when the As was synthesized by the de novo translated Rep (Figure 3B). Because the Rep was translated linearly over time (Figure S5) and the antisense strands were also synthesized linearly when Rep was added (Figure S6), then As synthesis by the de novo translated Rep should be proportional to the time squared. Therefore, we fitted the time-course data with Equation (1):

$$[As_t] = a^{\text{exp}}(t - t_{\text{lag}})^2 + b \quad (1)$$

where  $[As_t]$  is the total antisense strand concentration at time  $t$ ;  $a^{\text{exp}}$  is the experimentally measured coefficient of  $t^2$  and represents the acceleration of As synthesis;  $t_{\text{lag}}$  is the lag time for the appearance of active Rep caused by the period required for the Rep to be translated; and  $b$  is a constant representing the background signal. Curve fitting was performed with  $a^{\text{exp}}$  as a variable parameter for both the Rib and sense RNA concentrations with  $t_{\text{lag}}$  and  $b$  as common parameters for all Rib concentrations and as a variable parameter for sense RNAs (Figure 3B). As a result,  $t_{\text{lag}}$  was similar for all sense RNAs, with values of 2.5, 2.6 and 3.1 min for MDV(+) $\beta$ (+), MDV(-) $\beta$ (+) and MDV(-)TR- $\beta$ (+), respectively. Values of  $a^{\text{exp}}$ , the coefficients of  $t^2$ , are plotted in Figure 3C (○). For

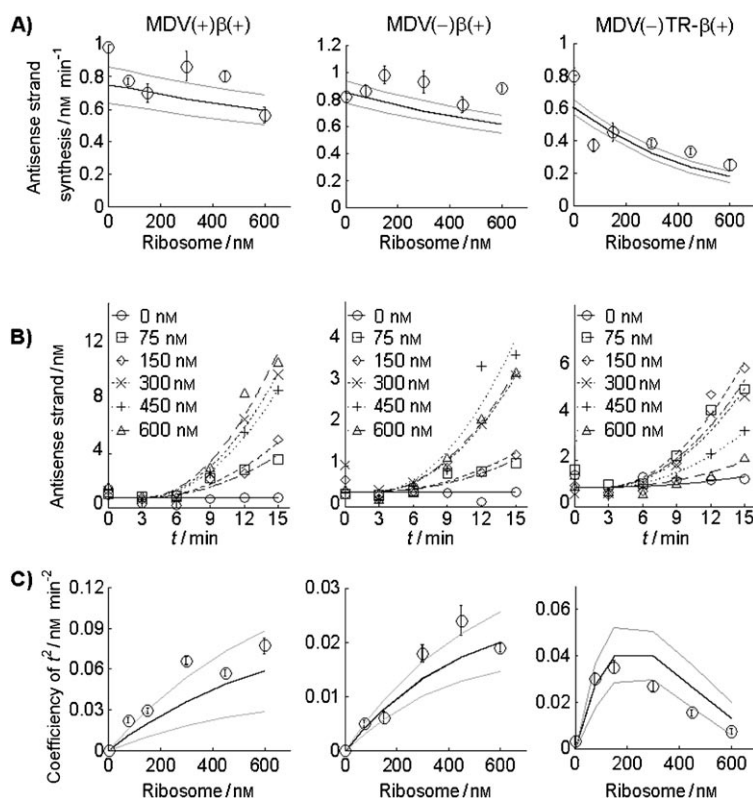


**Figure 3.** Antisense strand (As) synthesis. The three columns show the results for MDV(+) $\beta$ (+), MDV(-) $\beta$ (+) and MDV(-)TR- $\beta$ (+). A) Antisense strand synthesis rates by purified Rep. Experimentally, As synthesis by the purified Rep (20 nM; the active fraction was approximately 20%) was measured at various Rib concentrations in the absence of the amino acids, serine and lysine (i.e., without translational elongation). The time-course curves (Figure S6) were subjected to linear regression, and the slopes were plotted for each sense RNA (○). The error bars indicate standard errors. Theoretically, the As synthesis rates were calculated from Equations (3), (5) and (6), with the parameters shown in Table 1 (black line). Theoretically calculated values  $\pm$  standard deviation lines are also shown (gray lines). B) Time-course curves of As synthesis by the de novo translated Rep. The results were fitted to Equation (1), and the experimentally measured coefficients of  $t^2$  ( $a^{\text{exp}}$ ) are plotted (C). The insets show Rib concentrations. C) Coefficients of  $t^2$ ; the experimental results are plotted (○). The theoretical equivalents of  $a^{\text{exp}}$ ,  $1/2k_{\text{cat}}^{\text{Rep}} \times \gamma \times \alpha^{\text{Rep}} \times V^{\text{Rep}}$ , were calculated from the parameters shown in Table 1 (black line). Theoretically calculated values  $\pm$  standard deviation lines are also shown (gray lines).

MDV(+) $\beta$ (+) and MDV(-) $\beta$ (+),  $a^{\text{exp}}$  increased as the Rib concentration increased. In contrast, the Rib concentration dependency of  $a^{\text{exp}}$  showed a bell-shaped curve for MDV(-)TR- $\beta$ (+); this indicates that an excess of Ribs inhibited the replication reaction.

We investigated whether the experimental results could be explained by the kinetic model with the competition effect. In the model,  $a^{\text{exp}}$  can be written as  $1/2k_{\text{cat}}^{\text{Rep}} \times \gamma \times \alpha^{\text{Rep}} \times V^{\text{Rep}}$  [Eq. (8)], as shown in the Experimental Section, when all parameters were already known (Table 1). The calculated  $a^{\text{exp}}$  values (black line) were close to the experimental data (○) for all sense RNAs examined; this indicates that the kinetic model with the competition effect sufficiently explained the experimental results of these sense RNAs. For MDV(-)TR- $\beta$ (+), the calculated  $a^{\text{exp}}$  values formed a bell-shaped curve as did the experimental results. According to the model, the inhibition of As synthesis by the Ribs for MDV(-)TR- $\beta$ (+) was mainly attributed to two factors: 1) the higher affinity of MDV(-)TR- $\beta$ (+) for Ribs (smaller



$K_M^{\text{Rib}}$  value), which increased the fraction of RNA capable of binding to Ribs, resulted in a more severe competition effect, and 2) decrease in the  $\alpha^{\text{Rep}}$  when the Rib concentration was increased (Table 1, legends). Note, that even if we assumed a constant  $\alpha^{\text{Rep}}$ , the calculated  $\alpha^{\text{exp}}$  values for MDV(-)TR- $\beta$ (+) showed a bell-shaped curve (Figure S7).

## Discussion

Herein, we demonstrated experimentally that in the self-encoding system, competition between the Rib and Rep for the sense RNA occurred and significantly affected antisense strand (As) synthesis. Although the self-encoding system has more than 100 gene products,<sup>[21]</sup> our kinetic model, which is characterized by a few parameters, explained both the Rep  $\beta$ -subunit translation rates and the As synthesis rates quantitatively (Figures 2 and 3). As shown in the bell-shaped curve (Figure 3C) for MDV(-)TR- $\beta$ (+), more translation did not simply result in more As synthesis in the self-encoding system because excessive Rib concentration inhibited As synthesis due to the competition effect. The As is the intermediate of RNA replication, and therefore, this result demonstrated that the balance between translation and replication was critical for efficient replication by the self-encoded Rep. From the kinetic model we were able to address the questions of the optimum Rib concentration for replication of RNA by the self-encoding Rep in the presence of competition. The results indicated that the optimum active Rib concentration is equal to  $K_M^{\text{Rib}}$ , when half of the RNAs are bound by Ribs and the other half are available for Rep (see the Supporting Information for the derivation). The  $K_M^{\text{Rib}}$  for MDV(-)TR- $\beta$ (+) was 22 nM (Table 1), and the experimentally measured optimum Rib concentration was 150 nM (Figure 3C). As the active Rib ratio was 0.17, the experimentally measured concentration of optimum active Rib was approximately 26 nM, which is close to the  $K_M^{\text{Rib}}$  value.

Replication of RNAs by Q $\beta$  Rep and the translation of some enzymes from the RNAs were reported previously.<sup>[31–33]</sup> The competition between the Rib and Rep has also been observed.<sup>[23,24]</sup> In these previous studies, translation of viral proteins and RNA synthesis by a Rep were measured in crude extracts,<sup>[31–33]</sup> in which unknown components and concentrations limited the quantitative analysis of the competition effect. In addition, the translation of Rep and the replication by the self-encoded enzyme did not occur simultaneously in these studies. Instead, the Rep was added externally, and thus, the effect of the competition for the self-encoding systems has not been evaluated. Herein, we used a pure, reconstituted, self-encoding system as an experimental model, in which we could control the concentration of all the components. Therefore, we were able to determine the parameters experimentally and present the kinetic model that explained the competition effect quantitatively. This is an advantage of a reconstructed system like an artificial cell.

Although the self-encoding system used here does not exist in nature, the kinetic model and concepts obtained herein would be applicable to other self-encoding systems, such as RNA virus replication. Indeed, during Q $\beta$  phage infection, both

the replication of the genome and translation of phage protein occur simultaneously and can compete for the RNA genome.<sup>[34]</sup> The kinetic model we constructed would contribute to the quantitative understanding of RNA phage replication systems, one of the self-encoding systems. It is of interest to examine whether the  $K_M^{\text{Rib}}$  values of phage genome RNA are optimized for replication at the cellular Rib concentration.

A number of researchers, including our group, are engaged in attempts to assemble an artificial cell,<sup>[1,2,5,21]</sup> however, several hurdles remain to be overcome. One of the difficulties lies in coordinating several reactions without disturbing any one of them.<sup>[4]</sup> Here, we examined the interaction of two reactions, translation and replication, and found the optimum conditions under which both processes work well. Although we used a self-encoding system composed of RNA and proteins, any self-encoding system should suffer from the same competition effect as long as information molecules have dual roles, the two roles are in competition and the two roles are played at high frequency. The results obtained herein should contribute to the construction of an artificial cell, including an efficient system for the replication of genetic information.

## Experimental Section

**Reagents:** The reconstituted in vitro translation system (PURE system) was purchased from Post-Genome Institute (Tokyo, Japan). Purified Q $\beta$  Rep was prepared as described previously.<sup>[29,35]</sup> The standard reaction mixture was the same as that described previously except that it contained sense RNA template (70 nM) and Ribs at the indicated concentrations.<sup>[21]</sup> The mixtures were incubated at 37 °C. The template RNAs were prepared by in vitro transcription from each plasmid.<sup>[29]</sup> Plasmid construction is described in the Supporting Information.

**Measurement of the antisense strand (As) and replicase (Rep)  $\beta$ -subunit concentrations:** Antisense RNA concentration was measured by strand-specific quantitative real-time PCR as described previously.<sup>[21]</sup> Curve fitting was performed with KaleidaGraph (Synergy, Reading, PA, USA) or GraphPad (Prism, San Diego, CA, USA). The translated Rep  $\beta$  subunit was quantified by [<sup>35</sup>S]-methionine incorporation (19 kBq  $\mu\text{L}^{-1}$ ; Amersham, Bucks, UK), followed by SDS-PAGE as described previously.<sup>[21]</sup>

**Equations [Eq. (2), (3), (4), (5) and (6)]:** From the kinetic model (Figure 1B) and the assumptions described in the text, the rates of the synthesis of Rep and As RNA were derived as shown below (for details, see the Supporting Information):

$$V^{\text{Rep}} = k_{\text{cat}}^{\text{Rib}} \cdot [\text{Rib} - S] \quad (2)$$

$$V^{\text{As}} = k_{\text{cat}}^{\text{Rep}} \cdot [\text{Rep} - S] \quad (3)$$

$$[\text{Rib} - S] = \frac{1}{2} (K_M^{\text{Rib}} + [S_t] + \alpha^{\text{Rib}} [\text{Rib}_t]) - \sqrt{(K_M^{\text{Rib}} + [S_t] + \alpha^{\text{Rib}} [\text{Rib}_t])^2 - 4[S_t]\alpha^{\text{Rib}} [\text{Rib}_t]} \quad (4)$$

$$[\text{Rep} - S] = \alpha^{\text{Rep}} [\text{Rep}_t] \cdot \gamma \quad (5)$$

$$\gamma = \frac{[\text{Rep} - S]}{\alpha^{\text{Rep}} [\text{Rep}_t]} = \frac{1}{\left(\frac{K_M^{\text{Rep}}}{([S_t] - [\text{Rib} - S])} + 1 + \frac{(\alpha^{\text{Rib}} [\text{Rib}_t] - [\text{Rib} - S])}{K_M^{\text{Rib}}}\right)} \quad (6)$$

$V^{\text{Rep}}$  and  $V^{\text{As}}$  are Rep translation and As synthesis rates, respectively;  $\alpha^{\text{Rep}}$  and  $\alpha^{\text{Rib}}$  are the active ratios of Rep and Rib, respectively;  $[S_t]$ ,  $[\text{Rep}_t]$  and  $[\text{Rib}_t]$  are the total concentrations of sense strand RNA, Rep and Rib, respectively; and  $\gamma$  is the ratio of Rep–RNA complex (Rep–S) to total Rep ( $\text{Rep}_t$ ), which indicates the magnitude of the competition effect. Increasing Rib concentration decreases  $\gamma$  and subsequently decreases  $V^{\text{As}}$  because the equilibrium moves to the Rib-bound form, which cannot be used for As synthesis, depending on the affinity of the Rib for sense RNA ( $K_M^{\text{Rib}}$ ). Note that the Rib can inhibit replication by reducing the  $\gamma$  value, whereas Rep does not inhibit translation under these experimental conditions because of the excess RNA in comparison to Rep.

As  $V^{\text{Rep}}$  is constant over time, total Rep concentration is given as follows [Eq. (7)]:

$$[\text{Rep}_t] = V^{\text{Rep}} \cdot t \quad (7)$$

Since  $\gamma$  and  $\alpha^{\text{Rep}}$  are constant over time, total antisense strand concentration ( $[\text{As}_t]$ ) is given by Equations (3), (5) and (7) as follows [Eq. (8)]:

$$[\text{As}_t] = \frac{1}{2} \cdot k_{\text{cat}}^{\text{Rep}} \cdot \gamma \cdot \alpha^{\text{Rep}} \cdot V^{\text{Rep}} \cdot t^2 \quad (8)$$

As shown in Equation (8), the concentration of total antisense strand (As) is proportional to  $t^2$  in our experiments because As synthesis rate is proportional to the Rep concentration, which increases linearly over time.

## Acknowledgements

We thank Dr. Yasuaki Kazuta for his technical advice regarding the PURE system. This research was partially conducted in Open Laboratories for Advanced Bioscience and Biotechnology (OLABB), Osaka University. This research was supported in part by "Special Coordination Funds for Promoting Science and Technology: Yuragi Project" and "Global COE (Centers of Excellence) Program" of the Ministry of Education, Culture, Sports, Science, and Technology, Japan.

**Keywords:** artificial cells · gene expression · Q $\beta$  replicase · RNA · translation

- [1] J. W. Szostak, D. P. Bartel, P. L. Luisi, *Nature* **2001**, *409*, 387–390.  
 [2] A. C. Forster, G. M. Church, *Mol. Syst. Biol.* **2006**, *2*, 45.  
 [3] D. Deamer, *Trends Biotechnol.* **2005**, *23*, 336–338.  
 [4] A. Pohorille, D. Deamer, *Trends Biotechnol.* **2002**, *20*, 123–128.

- [5] P. L. Luisi, *Anatom. Rec.* **2002**, *268*, 208–214.  
 [6] M. M. Hanczyc, S. M. Fujikawa, J. W. Szostak, *Science* **2003**, *302*, 618–622.  
 [7] I. A. Chen, J. W. Szostak, *Proc. Natl. Acad. Sci. USA* **2004**, *101*, 7965–7970.  
 [8] S. S. Mansy, J. P. Schrum, M. Krishnamurthy, S. Tobe, D. A. Treco, J. W. Szostak, *Nature* **2008**, *454*, 122–125.  
 [9] D. P. Bartel, P. J. Unrau, *Trends Cell Biol.* **1999**, *9*, M9–M13.  
 [10] U. F. Müller, *Cell. Mol. Life Sci.* **2006**, *63*, 1278–1293.  
 [11] A. C. Chakrabarti, R. R. Breaker, G. F. Joyce, D. W. Deamer, *J. Mol. Evol.* **1994**, *39*, 555–559.  
 [12] T. Oberholzer, R. Wick, P. L. Luisi, C. K. Biebricher, *Biochem. Biophys. Res. Commun.* **1995**, *207*, 250–257.  
 [13] T. Oberholzer, K. H. Nierhaus, P. L. Luisi, *Biochem. Biophys. Res. Commun.* **1999**, *261*, 238–241.  
 [14] K. Ishikawa, K. Sato, Y. Shima, I. Urabe, T. Yomo, *FEBS Lett.* **2004**, *576*, 387–390.  
 [15] V. Noireaux, A. Libchaber, *Proc. Natl. Acad. Sci. USA* **2004**, *101*, 17669–17674.  
 [16] T. Sunami, K. Sato, T. Matsuura, K. Tsukada, I. Urabe, T. Yomo, *Anal. Biochem.* **2006**, *357*, 128–136.  
 [17] D. S. Tawfik, A. D. Griffiths, *Nat. Biotechnol.* **1998**, *16*, 652–656.  
 [18] P. L. Luisi, F. Ferri, P. Stano, *Naturwissenschaften* **2006**, *93*, 1–13.  
 [19] U. F. Müller, D. P. Bartel, *RNA* **2008**, *14*, 552–562.  
 [20] T. Oberholzer, M. Albrizio, P. L. Luisi, *Chem. Biol.* **1995**, *2*, 677–682.  
 [21] H. Kita, T. Matsuura, T. Sunami, K. Hosoda, N. Ichihashi, K. Tsukada, I. Urabe, T. Yomo, *ChemBioChem* **2008**, *9*, 2403–2410.  
 [22] T. Blumenthal, G. G. Carmichael, *Annu. Rev. Biochem.* **1979**, *48*, 525–548.  
 [23] D. Kolakofsky, C. Weissmann, *Nat. New Biol.* **1971**, *231*, 42–46.  
 [24] D. Kolakofsky, C. Weissmann, *Biochim. Biophys. Acta Nucleic Acids Protein Synth.* **1971**, *246*, 596–599.  
 [25] C. K. Biebricher, M. Eigen, W. C. Gardiner, Jr., *Biochemistry* **1984**, *23*, 3186–3194.  
 [26] M. Eigen, C. K. Biebricher, M. Gebinoga, W. C. Gardiner, *Biochemistry* **1991**, *30*, 11005–11018.  
 [27] J. T. August, A. K. Banerjee, L. Eoyang, M. T. Franze de Fernandez, K. Hori, C. H. Kuo, U. Rensing, L. Shapiro, *Cold Spring Harb. Symp. Quant. Biol.* **1968**, *33*, 73–81.  
 [28] M. Werner, *Biochemistry* **1991**, *30*, 5832–5838.  
 [29] K. Hosoda, T. Matsuura, H. Kita, N. Ichihashi, K. Tsukada, T. Yomo, *J. Biol. Chem.* **2007**, *282*, 15516–15527.  
 [30] D. L. Kacian, D. R. Mills, F. R. Kramer, S. Spiegelman, *Proc. Natl. Acad. Sci. USA* **1972**, *69*, 3038–3042.  
 [31] L. Ryabova, E. Volianik, O. Kurmasov, A. Spirin, Y. Wu, F. R. Kramer, *J. Biol. Chem.* **1994**, *269*, 1501–1505.  
 [32] I. Y. Morozov, V. I. Ugarov, A. B. Chetverin, A. S. Spirin, *Proc. Natl. Acad. Sci. USA* **1993**, *90*, 9325–9329.  
 [33] V. I. Ugarov, I. Morozov, G. Y. Jung, A. B. Chetverin, A. S. Spirin, *FEBS Lett.* **1994**, *341*, 131–134.  
 [34] E. Vinuela, I. D. Algranati, S. Ochoa, *Eur. J. Biochem.* **1967**, *1*, 3–11.  
 [35] H. Kita, J. Cho, T. Matsuura, T. Nakaishi, I. Taniguchi, T. Ichikawa, Y. Shima, I. Urabe, T. Yomo, *J. Biosci. Bioeng.* **2006**, *101*, 421–426.

Received: July 31, 2008

Published online on November 19, 2008